IPPI
Polyolefins Journal, Vol. 12, No. 3 (2025)
DOI: 10.22063/poj.2025.35680.1355
ORIGINAL PAPER

Nanostructure refining of polypropylene/nanoclay composite via optimization of compatibilizer and masterbatch parameters

Negin Sadat Jalili, Bahereh T. Marouf, Ali Bakhshi-Zadeh, Reza Bagheri*

Polymeric Materials Research Group (PMRG), Department of Materials Science and Engineering, Sharif University of Technology, Azadi Ave., Tehran, IR

Received: 9 April 2025, Accepted: 17 July 2025

ABSTRACT

The aim of the current study was to first make two compatibilizers, i.e., maleic anhydride-grafted polypropylene (PP-g-MA), based on a homo-and a block copolymer. Then, these custom compatibilizers were incorporated into PP/nanoclay composites made via direct and two-step masterbatch techniques. The influence of compatibilizer/nanoclay ratio was examined into the direct method. In the two-step processing technique, the compatibilizer content was divided into two parts such that the first part was used when making the masterbatch and the second part was incorporated in the second step when the masterbatch was diluted by the polymer matrix. The characterizations via titration test and Fourier-transform infrared (FTIR) spectroscopy revealed a higher degree of grafting reaction when homo-polymer was used for synthesizing PP-g-MA. In the next step, nanocomposites containing 3 wt.% nanoclay with three different PP-g-MA (both types)/nanoclay ratios of 1:1, 2:1, and 3:1 were made using a co-rotating twin screw extruder. X-ray diffraction (XRD) analysis was done to evaluate morphology and tensile and impact properties, and tests were performed to evaluate the mechanical properties of the PP samples. Based on the results, maleic anhydride-grafted homo-polypropylene (HPP-g-MA) and the composition containing HPP-g-MA/nanoclay ratio of 2:1 with 7.69% improvement in Young's modulus was reported as the recommended compatibilizer and ratio for applications. Finally, five nanocomposite samples with identical composition were made in two steps. A masterbatch containing 15 wt.% nanoclay was made first and then, it was diluted with PP to reduce the nanoclay content to 3 wt.%. All samples contained 6 wt.% PP-g-MA, but the method of addition of compatibilizer was different. In one sample, the whole compatibilizer was added into the masterbatch. In another sample, the entire PP-g-MA was added in the second stage of compounding. In the other three samples, the addition of compatibilizer was divided between the two stages of the process. The results of the study showed that the highest improvement of elastic modulus (24.26%) was obtained when the majority of the compatibilizer was added in the second step of production. This was associated with the best dispersion of nanoclay platelets in the PP matrix. **Polyolefins J (2025) 12: 175-189**

Keywords: Mechanical properties; masterbatch; compatibilizer; polypropylene; nanoclay.

INTRODUCTION

Polypropylene (PP), due to its versatility, low price, low density and reasonable mechanical properties is amongst the most consumed thermoplastics [1,2]. Still, the need for improvement of its mechanical properties has driven researchers to examine different kinds of modifiers and reinforcements in this polymer. Along this line, the incorporation of nanoclay into PP has been tried by many investigators over the past two decades [3-6].

Researchers have tried different approaches to obtain PP/nanoclay composites with uniform distribution and dispersion of exfoliated nanoclay platelets [7]. Due to the difference in the nature of nanoclay and polypropylene, i.e., the first one being polar while the latter is non-polar, some sort of compatibilization between the two components is required in a blend. This is usually done by modification of the pristine clay to form "organoclay" and also utilization of a kind of compatibilizer in the blending step [8]. The role of compatibilizer is to add polar moieties to the matrix to enhance nanometric distribution and dispersion of clay

*Corresponding Author - E-mail: rezabagh@sharif.edu

platelets throughout the matrix. Maleic anhydride-grafted polypropylene (PP-g-MA) is the most used compatibilizer in these studies [9]. This is made via reactive blending of polypropylene and maleic anhydride in the presence of an initiator, commonly used dicumyl peroxide (DCP) [10-12]. It is well known that the degree of grafting of MA to PP chains, which depends on the MA content and the initiator used, contributes to the effectiveness of the compatibilizer [13-15]. However, not much information has been reported on the role of the type and characteristics of the polypropylene used in synthesizing PP-g-MA.

A vast number of investigations have examined the effect of type and concentration of nanoclay and compatibilizer on the mechanical performance in PP/nanoclay composites. There is a general agreement that tensile strength and elastic modulus of the composite increase by organoclay content as far as a uniform distribution and dispersion of the platelets exists and that the impact strength declines under such circumstances [10,11]. The influence of the ratio of compatibilizer to nanoclay on the engineering properties of PP/nanoclay composites has been the subject of some research as well [12,16,17]. While there is no strong agreement in this regard, the majority of the literature illustrates that the optimum compatibilizer content must be between two and three times that of the nanoclay loading [18]. Further addition of compatibilizer has shown to have a negative effect on mechanical properties of the nanocomposite [18].

In order to obtain a more uniform nanostructure, investigators have employed a two-(or even multiple-) step fabrication method [17,19]. According to this approach, a masterbatch of the nanoclay is made in the first step. In the following step, the masterbatch is diluted by the matrix resin to reach the desired nanoclay content. The two-step process, usually done by means of twin-screw extruders, results in better distribution and dispersion of nanoclay platelets. Thus, higher strength and stiffness of the nanocomposite can be obtained [17,18,20]. Rama *et al.* [20] reported that the interlayer spacing of the nanoclay platelets was larger when the masterbatch technique was implemented. This observation, in turn, was associated with higher Young's modulus and yield strength of the nanocomposite.

When using the two-step masterbatch technique, a question could arise about whether the investigator should incorporate the compatibilizer in the first step of compounding or when diluting the masterbatch with the polymer matrix. It may be argued that the compatibilizer could be introduced in both steps as well. As a matter of fact, different researchers who tried the two-step technique acted differently. While some of them employed the entire compatibilizer content in one step [19,21-23], some divided their compatibilizer into two parts and incorporated each part in each step of processing [24]. Despite plenty of research has examined the two-step approach, there is no consensus in the literature about the influence of dividing the compatibilizer content into two parts. This is due to the lack of systematic studies in this regard. What makes the scenario even more complicated is that in a major part of studies, commercial compatibilizers have been employed and thus, the results might have been affected by the unknown nature of the polypropylene used in synthesizing the compatibilizer.

The goal of the current study is to first make two compatibilizers, i.e. PP-g-MA, based on a homo-and a block copolymer. Then, these custom compatibilizers will be incorporated into PP/nanoclay composites made via direct and two-step masterbatch techniques. The influence of compatibilizer/nanoclay ratio will be examined in the direct method. In the two-step processing technique, the compatibilizer content will be divided into two parts such that the first part will be used when making the masterbatch and the second part will be incorporated in the second step when the masterbatch is diluted by the polymer matrix.

EXPERIMENTAL

Materials

The materials used in this study are listed in Table 1. Co-polypropylene EP440L was chosen as the matrix for the nanocomposites, while two types of co-polypropylene, EP548R, and homo-polypropylene with the trade name of HP552R were used as the base material for maleic anhydride compatibilizers. A co-polypropylene, 548T, was utilized as the base polymer for masterbatches. An organoclay with the trade name of Nanolin DK4 was selected as nanoclay filler for incorporation into the PP matrix.

Compatibilizer synthesis

As mentioned, two types of PP, HP552R homo-polypropylene (HPP) and EP548R co-polypropylene (CPP), with almost identical melt flow indices (MFIs) were used for synthesis of compatibilizers to determine the influence of base polymer. First, 4 wt.% of MA along with 0.05 wt.%. DCP was dissolved in

Table 1. Materials used in this study.

Material	Commercial name	Supplier	MFI* (g/10 min)
Nanoclay	DK4	FCC Inc.	-
Co-polypropylene	EP440L	Jampilen	6
Co-polypropylene	548T	Jampilen	50
Co-polypropylene	EP548R	Jampilen	21
Homo-polypropylene	HP552R	Jampilen	23
Maleic anhydride	-	Merck	-
DCP	-	Merck	-
Xylene	-	Neutron	-

*Melt flow index (MFI) measurements were done using a 2.16 kg weight at 230°C.

acetone, and then, polymer pellets were added to the solution. The mixture was stirred until the acetone vaporized, and white deposits appeared on the surface of PP pellets. Compositions of the two synthesized compatibilizers are given in Table 2. Grafting of MA to PP chains was achieved by extruding the mixture with a SHJ-20 Nanjing Giant intermeshing co-rotating twin-screw extruder with L/D = 20 and screw speed of 300 rpm at 200°C for all extruder zones. The residence time in the extruder was approximately 1 min based on screw speed, feed rate, and extruder dimensions, which has been reported as sufficient for maleic anhydride grafting reactions under comparable conditions, particularly when using DCP as an initiator [25]. It should be noted that residence time in extrusion inherently exhibits a distribution; however, due to equipment limitations, direct characterization of the residence time distribution (RTD) was not feasible in this study.

Preparation of nanocomposites via direct method

Compositions of the nanocomposites made via direct method are mentioned in Table 3. As seen, the compatibilizer/nanoclay ratio was varied in this set of experiments. Direct melt blending of the constituents was done using the same twin-screw extruder mentioned in section 2.2. Before the extrusion, a TURBULA® shaker-mixer was employed to pre-mix the constituents. Then the pre-mixed materials were

Table 2. Designations and compositions of the synthesized compatibilizers used in this study.

Compatibilizer designation	Base polymer	DCP content (wt.%)	MA content (wt.%)	Base polymer content (wt.%)
CPP-g-MA	EP548R	0.05	4	95.95
HPP-g-MA	HP552R	0.05	4	95.95

extruded. The temperature profile of the extruder was set at 200-200-200-190°C along the barrel. EP440L CPP with MFI of 6 g/10 min was incorporated as the polymer matrix for making nanocomposite samples.

Preparation of nanocomposites via two-step masterbatch method

Based on the results of the evaluations of compatibilizers synthesized and nanocomposites made in a one-step approach, as will be shown later, HPP-g-MA was used as the compatibilizer and the compatibilizer/nanoclay ratio of 2 was selected for making this set of samples. Therefore, according to the original plan of the research, the compatibilizer content was divided into two parts such that the first part was incorporated in making masterbatches, as shown in Table 4. The rest of the compatibilizer content was then added to the compound when diluting the masterbatch, according to Table 5. Please note that all the compounds made in this step contain 3 wt.% nanoclay and 6 wt.% compatibilizer. In the case of PC1 compound in Table 5, for example, the entire compatibilizer has been added in the second step of diluting the masterbatch. In the case of PC5, however, the entire compatibilizer has been incorporated into the masterbatch.

The processing technique for making the masterbatches and the compounds were identical to that introduced in section 2.3. The base resin for making the masterbatches was a co-polypropylene; 548T with a high MFI of 50 g/10 min. Similar to the one-step approach, the base polymer for the compounds was EP440L. The reason for choosing a resin with a high

Table 3. Designations and compositions of nanocomposites processed via the direct mixing method.

Designation	Compatibilizer	Nanoclay content (wt.%)	Compatibilizer content (wt.%)	Compatibilizer/ nanoclay ratio
H11	HPP-g-MA	3	3	1
H21	HPP-g-MA	3	6	2
H31	HPP-g-MA	3	9	3
C11	CPP-g-MA	3	3	1
C21	CPP-g-MA	3	6	2
C31	CPP-g-MA	3	9	3

Table 4. Designations and compositions of the masterbatches processed for the two-step process.

Designation	Nanoclay content (wt.%)	Compatibilizer* content (wt.%)	Base polymer** content (wt.%)
MB1	20	0	80
MB2	20	13.33	66.67
MB3	20	20	60
MB4	20	26.67	53.33
MB5	20	40	40

*Compatibilizer used in this step is HPP-g-MA (see Table 2).
**Base polymer used for masterbatch preparation is 548T CPP with MFI = 50 g/10 min.

MFI as the base for the masterbatches was their ease of processing as well as improved dispersion of nanoclay platelets in the final compositions.

Furthermore, to evaluate the effect of compatibilizer and base polymer of masterbatches without organoclay on the mechanical properties of EP440L co-PP, two additional samples, namely PP+HPP-g-MA and PP+PP-MB, were processed using direct mixing in one-step method. PP+HPP-g-MA is a compound of 94 wt.% EP440L co-PP and 6 wt.% of HPP-g-MA compatibilizer similar to the composition of the nanocomposites processed using direct process. On the other hand, the amount of 548T in two-step processed nanocomposites varied and PC1 contained the largest amount of 548T with 12 wt.%. Thus, PP+PP-MB containing 88 wt.% EP440L co-PP and 12 wt.% of 548T co-PP was prepared to characterize the effect of masterbatches' base polymer on the mechanical properties of the nanocomposites studied in this investigation.

Preparation of test samples

In order to analyze the synthesized compatibilizers, the procedure done by Pruthtikul and Liewchirakorn [11] was used. According to this approach, the first excessive MA that did not participate in the grafting reaction was removed. To do this, 5 g of each compatibilizer was separately dissolved in 100 ml of xylene at 140-160°C on a stirrer. After that, the solution was cooled down to room temperature. Next, acetone was added to the solution gradually and the compatibilizer deposited as white sediments. Using a filter paper, these sediments were separated and then dried in an air circulating oven for 3 hours at 105°C. The resulting powder was used for titration, Fourier-transform infrared (FTIR), and differential scanning calorimetry (DSC) tests.

Nanocomposites fabricated with extrusion process were pelletized and then injection molded to standard dumbbell specimens according to ISO 527 testing protocol using a FU CHUN SHIN (model HT-100) injection molding apparatus at 210°C. These specimens were used for tensile, impact, X-ray diffraction (XRD), scanning electron microscopy (SEM), and rheological examinations.

Characterizations

Titration, FTIR, MFI and rheological analysis of compatibilizers

The MA reaction degree was evaluated by titration and measuring the acid number parameter [11]. First, 0.5 g of refined compatibilizer powder was dissolved in 50 ml of xylene in 140-160°C. Then a few drops of distilled water were added to the solution for hydrolysis. Thymol Blue was used as an indicator and the titrating solution was methanol solution containing 0.05 mol KOH [26]. According to Equation 1, the acid number of compatibilizer can be obtained from required KOH solution volume used for titration:

$$Acid\ number\ (A.N.) = \frac{56.1 \times N \times V}{g} \quad (1)$$

where N is KOH solution concentration, V is the volume of KOH solution in the endpoint of titration and g is the mass of initially dissolved compatibilizer in xylene.

Based on the acid numbers for the two compatibilizers,

Table 5. Designations and compositions of nanocomposites processed via the two-step masterbatch method.

Designation	Masterbatch used	Masterbatch content† (wt.%)	Compatibilizer* content (wt.%)	Base polymer** content (wt.%)
PC1	MB1	15	6	79
PC2	MB2	15	4	81
PC3	MB3	15	3	82
PC4	MB4	15	2	83
PC5	MB5	15	0	85

†Base polymer used in masterbatch preparation is 548T CPP with MFI = 50 g/10 min.
*Compatibilizer content refers to the amount added in the second compounding step.
**Matrix polymer used in final compounds is EP440L CPP with MFI = 6 g/10 min.

MA content can be calculated from the below relation:

$$MA\ content = \frac{Acid\ number \times M_{MA}}{2 \times 1000} \quad (2)$$

where MMA, molar mass of maleic anhydride, is 98.06 g/mol.

The FTIR analysis was performed on a Bruker model Tensor 27 analyzer. Based on Equation 3, the ratio of the area over these peaks (also known as Carbonyl index) can be employed as a criterion to compare how much grafting reaction has proceeded:

$$\text{Carbonyl index (C.I.)} = \frac{A_{1780}}{A_{1160}} \quad (3)$$

MFI of compatibilizers were measured using a Gotech machine at 230°C and 2.16 kg weight.

Rheological behavior of the compatibilizers was studied through frequency sweep measurements done by Anton Paar testing device at 170°C in the 1-1000 s^{-1} frequency range, according to PP25-SN13969 testing protocol.

Differential scanning calorimetry (DSC)

DSC tests were performed using a TA-Q100 device according to ASTM 3418-03. To remove the thermal history of samples, all of them were first cycled from -20 to 220°C and turned back to -20°C at a heating and cooling rate of 10°C/min. The samples were finally heated up to 220°C at the same heating rate of 10°C/min for measuring melting temperature (T_m), and degree of crystallization. To calculate the percentage of crystallization ($\%X_c$), Equation 4 was used, in which ΔH°_f is the standard enthalpy of melting of fully crystallized PP with the value of 209 J/g, and ΔH_f is sample's melting enthalpy determined from DSC thermographs.

$$\%X_c = \frac{\Delta H_f}{\Delta H^\circ_f} \quad (4)$$

XRD and SEM analysis of nanocomposites

XRD patterns were obtained to verify the crystalline structure of the nanocomposites, average interlayer spacing in nanoclay platelets, and thickness of the nanoclay stacks in the nanocomposites. Tests were performed using a Philips Xpert PRO device and Cu K_α beam with a wavelength of 1.54 Å.

Dispersion of the nanoclay platelets was examined by TeScan model Mira III scanning electron microscope. For SEM, the fracture surfaces of the impact specimens after impact loading were considered. To prepare the microscopy specimens, the cross-sections of the specimen fracture surfaces were coated with a thin layer of gold to avoid charge build-up.

Mechanical tests

Tensile tests were conducted according to ISO 527 utilizing a Hounsfield Universal testing frame on standard specimens at the crosshead speed of 5 mm/min. For each formulation, five specimens were tested. Charpy impact tests were performed based on ISO 179 test method using a FT-7045-MD Gotech impact tester with a 2 J hammer. At least five notched specimens of each formulation were tested under impact loading in order to assure validity of the measurements.

Statistical analyses were performed using one-way analysis of variance (ANOVA) to determine the significance of differences in the mechanical properties including Young's modulus, yield strength, and impact strength outcomes between formulated systems. A significance level of $p < 0.05$ was considered a statistically meaningful value. All value are reported as mean ± standard deviation (SD).

RESULTS AND DISCUSSION

Evaluation of compatibilizers

Titration, MFI and rheological tests

Table 6 presents the results of titration and MFI measurements conducted on the synthesized compatibilizers, i.e., HPP-g-MA and CPP-g-MA. The HPP-g-MA sample consumed a larger volume of KOH solution during titration, resulting in a higher acid number. The lower acid number of CPP-g-MA indicates that it contains fewer MA moieties compared to HPP-g-MA, suggesting a higher degree of MA grafting onto HPP chains. This trend is consistent with the calculated MA contents reported in Table 6. Consequently, HPP-g-MA is expected to offer improved performance as a compatibilizer for dispersing clay platelets within the polypropylene matrix.

Although 4 wt.% of MA was initially introduced during the grafting process (Table 2), the actual grafted MA content measured in the modified PP ranged from 0.138 to 0.192 wt% (Table 6), indicating a relatively low grafting efficiency. This phenomenon is well documented in the literature and can be attributed to several interrelated factors. First, MA has a high vapor pressure at processing temperatures,

Table 6. Titration results, MFI and FTIR analysis of the synthesized compatibilizers.

Compatibilizer	KOH needed for titration (ml)	Acid number (mg KOH/g polymer)	MA content (wt.%)	MFI* (g/10min)	Carbonyl index**
HPP-g-MA	0.7 ± 0.05	3.927 ± 0.281	0.192 ± 0.014	70.02 ± 8.35	0.1337
CPP-g-MA	0.5 ± 0.05	2.805 ± 0.281	0.138 ± 0.014	39.01 ± 3.12	0.0821

*MFI measured at 230°C with using a 2.16 kg load.

**Carboxyl index (CI) calculated as A_{1780}/A_{1160}

leading to partial volatilization before it can react with the polymer backbone. Second, MA is prone to homopolymerization under radical conditions-particularly in the presence of peroxide initiators-which consumes MA and limits its availability for grafting onto PP. Third, side reactions such as β-scission, chain transfer, and radical termination can further reduce grafting efficiency by diverting reactive species from the grafting pathway. Additionally, the chemical structure of PP-dominated by relatively inert C–H bonds-limits the number of active sites for effective radical grafting. The presence of tertiary carbon atoms is critical for initiating grafting, but their availability is constrained in isotactic PP.

Processing parameters, including initiator concentration, temperature, mixing intensity, and residence time, also play crucial roles in determining grafting efficiency. For instance, excessive initiator loading can accelerate radical decomposition and increase chain degradation rather than enhance grafting. These limitations highlight the need for careful optimization of reaction conditions and formulation parameters to improve grafting efficiency, which is essential not only for enhancing interfacial compatibility and mechanical performance but also for minimizing cost and reducing residual unreacted MA or its homopolymers in the final material.

According to Table 6, the average melt flow index of HPP-g-MA was measured 70 g/10 min, while this quantity was obtained 39 g/10 min for CPP-g-MA. Comparing the melt flow indices of the two compatibilizers (Table 6) with those of their base polymers (Table 1) implies the occurrence of much more chain scission during synthesizing of HPP-g-MA. This observation seems to be in agreement with higher degree of MA grafting in PP-g-MA. This can be explained as follows. In the literature, it has been reported that the DCP initiator causes the scission of the polymer chain, thereby increasing the melt flow index of the polymer [27]. This phenomenon is well-documented, especially in the context of peroxide-induced degradation of PP using DCP, which promotes chain scission reactions over crosslinking under specific processing conditions (e.g., low concentration, high temperature, presence of oxygen). Subsequently, MA is connected to these broken regions on the polymer chain. In Table 6, it is observed that the melt flow index of compatibilizer HPP-g-MA, which has homo-polypropylene as its base polymer, is higher than that of compatibilizer CPP-g-MA, which has polypropylene copolymer as its base polymer. The amount of DCP used in both samples is identical; thus, it can be concluded that the effect of this initiator on homo-polypropylene is more pronounced than on polypropylene copolymer. In other words, the polyethylene present in polypropylene copolymer somehow hinders chain scission by DCP, resulting in a lesser increase in melt flow index for CPP-g-MA compared to the other sample.

Briefly, it can be concluded that as the degree of grafting increases, specifically from the data in Table 6 regarding MA to the polypropylene chain and as the acid number of the compatibilizer rises, the melt flow index of the compatibilizer also increases.

The results of rheological evaluation of the compatibilizers are seen in Figure 1. As seen in Figure 1a, the complex viscosity values of CPP-g-MA at 200°C are higher than that of HPP-g-MA for a very wide range of angular frequencies. This is in agreement with the MFI measurements reported in Table 6. The crossover of the two plots in Figure 1a at higher frequencies due to the steeper decrease of complex viscosity of CPP-g-MA compared to that of HPP-g-MA can be attributed to the wider molecular weight distribution in this material. Since the rheological behavior of the base polymer of the compatibilizers was not examined, it is not possible to judge that this wide molecular weight distribution has been associated with the grafting process or has existed from the beginning.

Figure 1b exhibits the dynamic storage and loss moduli versus angular frequency plots of HPP-g-MA and CPP-g-MA at 200°C. Higher moduli of CPP-g-MA and the crossovers in the upper right corner of the plots, again shows higher molecular weight and wider molecular weight distribution of CPP-g-MA

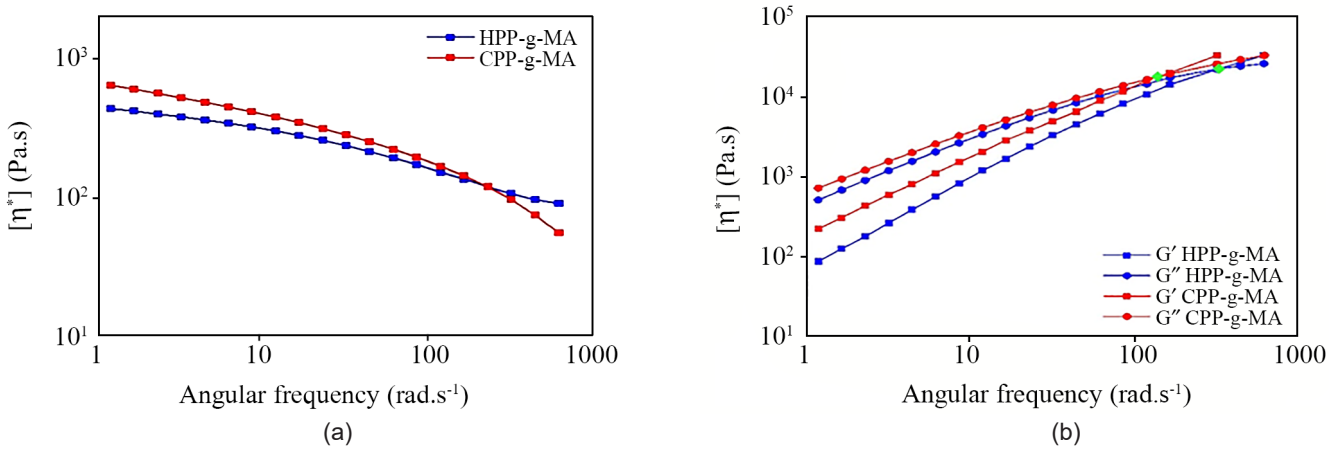

Figure 1. (a) Complex viscosity (η*) and (b) storage (G') and loss (G") moduli as a function of angular frequency (ω) for the synthesized compatibilizers.

compared to those of HPP-g-MA. As a result, it is expected that the compatibilizer HPP-g-MA with a lower molecular weight will be able to penetrate between the clay layers more easily compared to the compatibilizer CPP-g-MA, therefore facilitating the opening of the nanoclay platelets.

FTIR measurements

FTIR measurements were conducted to confirm and compare the extent of MA incorporation into the polypropylene chain. The results of FTIR measurements are illustrated in Figure 2. The peaks corresponding to the wave numbers 1160 and 1780 cm^{-1} are representatives of the CH_3 group and C=O bond associated with MA, respectively. The ratio of the areas of these two peaks serves as a criterion for comparing the degree of MA incorporation into polypropylene. In other words, the carbonyl index which is calculated by the ratio of the surfaces of 1780 to 1160 cm^{-1} is an indication of MA grafting. The calculated area ratios for both compatibilizers are listed in Table 6, allowing for a comparison of carbonyl index and percentage of MA incorporation into PP between these two samples. This ratio is 0.1337 and 0.0821 for HPP-g-MA and CPP-g-MA, respectively (Table 6). This observation confirms a higher degree of grafting of MA in HPP-g-MA, which agrees with the titration results.

DSC Analysis

The DSC results, including melting temperature and percentage crystallinity values of two compatibilizers (HPP-g-MA, CPP-g-MA) processed in this research, are presented in Table 7. However, the glass transition temperature was not reported because it was not measured during the DSC analysis. The DSC measurements were performed with heating cycles starting from −20°C, which is not enough below the typical Tg range of PP (generally around −20 to 0°C). As a result, the Tg was not obtained within the scanned temperature range and could not be reliably reported. As shown, the melting temperature of HPP-g-MA is 159.82°C, which is slightly lower than that of CPP-g-MA at 162.56°C. Additionally, the crystallinity percentages of HPP-g-MA and CPP-g-MA were found to be 37.28% and 31.19%, respectively. This difference in the crystallinity appears to be related to structural differences in the base polymer chains of the compatibilizers and the varying performance of DCP in the two samples. The co-polypropylene, the base polymer of CPP-g-MA compatibilizer, contains elastomer phases dispersed in the PP matrix, exhibiting a lower percent crystallinity than that of the homo-polypropylene, which is the base polymer of HPP-g-MA. On the other hand, referring back to the MFI outcomes, the DCP caused more degradation and chain scission in HPP-g-MA compared to its performance

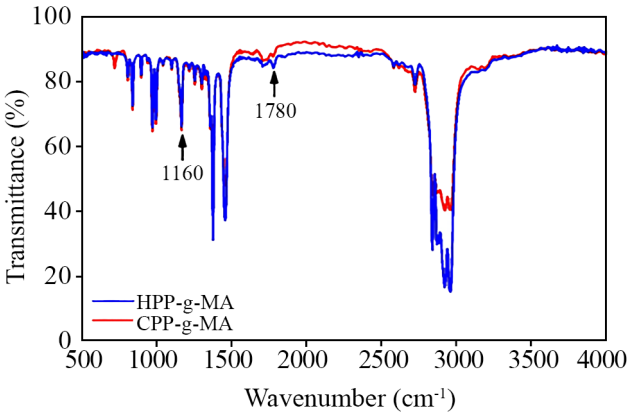

Figure 2. FTIR spectra of HPP-g-MA and CPP-g-MA compatibilizers.

Table 7. DSC results of the synthesized compatibilizers.

Designation	T_m (°C)	ΔH_f (J/g)	Crystallinity (%)
HPP-g-MA	160	77.91	37.3
CPP-g-MA	163	65.19	31.2

in the CPP-g-MA. Therefore, this shortening of the HPP-g-MA chain length may have contributed to their increased order, thus leading to a higher crystallinity percentage for compatibilizer HPP-g-MA compared to CPP-g-MA.

Evaluation of the nanocomposites made via direct method

Six nanocomposites made via direct method, H and C series (Table 3), along with the as received nanoclay were subjected to XRD analysis to evaluate the dispersion of nanoclay platelets in composites through examination of the XRD spectra and the d-spacing between the silicate layers. Figure 3 illustrates the XRD patterns of the mentioned samples and the calculated values from the spectra are reported in Table 8.

When analyzing the XRD results, attention has been paid to both displacing of 2θ peaks and thus the change in d-spacing between the layers and also the intensity of the peaks. Please note that the weight of the nanocomposite samples in this series of tests was identical. Therefore, the intensity of a given peak may represent, to some extent, the fraction of the corresponding layers. The XRD patterns display slight reductions in diffraction angles in clay-PP formulations, corresponding to slight increases in the d-spacing between clay platelets, suggesting intercalation of clay within the PP matrix. Table 8 shows the maximum increase in d-spacing of the silicate layers in C31and H31, for the C and H series, respectively. This finding alone may guide the reader to the point that probably the best nanoclay dispersion must have occurred in these two samples. However, a more precise look at the XRD spectra illustrates the minimum intensity of the peaks for C31 and

Table 8. XRD results for nanocomposites processed via the direct mixing method.

Sample	$\overline{2\theta}$ (°)	$\bar{d}$(Å)
DK4	2.49	35.45
C11	2.44	36.18
C21	2.38	37.09
C31	2.30	38.38
H11	2.42	36.48
H21	2.46	35.88
H31	2.31	38.21

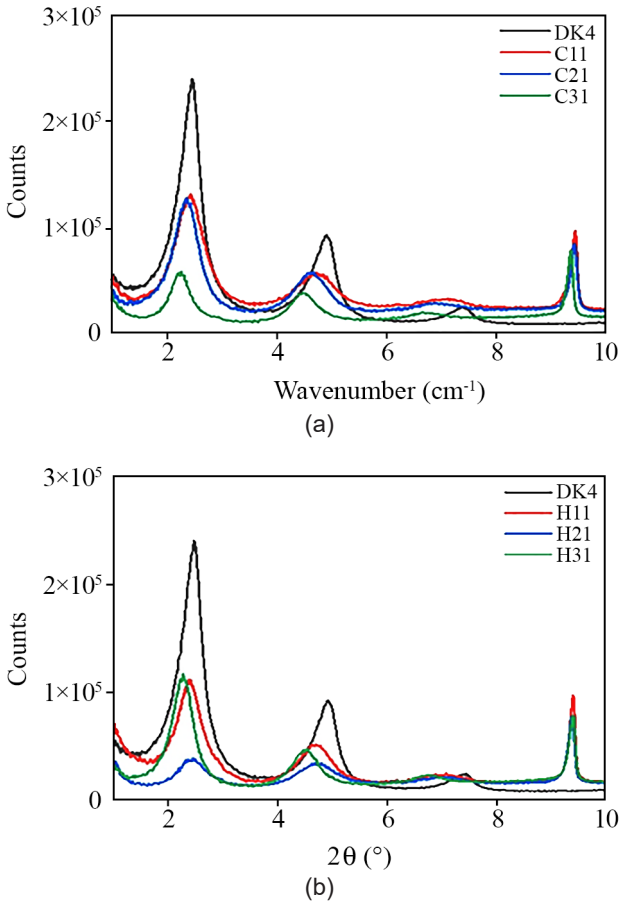

Figure 3. XRD patterns of nanocomposites processed via the direct mixing method using: (a) CPP-g-MA and (b) HPP-g-MA as compatibilizer. All samples contain 3 wt.% organoclay.

H21. Significant drop in the intensity of the peaks of these two samples suggests that possibly part of nanoclay platelets in these samples are exfoliated and thus, do not diffract X-ray. TEM assessments, as a supplementary technique, are required to confirm the partial exfoliation of clay platelets within the matrix. If this conclusion is true, one may expect to see the maximum increase in elastic modulus in C31 and H21, for the C and H series, respectively. Please note that the better the dispersion of the nanoclay platelets, the higher the elastic modulus of the nanocomposite [7]. Future work may include the uncompatibilized nanocomposite as a control to more precisely isolate the role of the compatibilizer in modulating clay structure. Furthermore, linear melt rheology measurements (not performed in this study) can provide valuable insights into filler-matrix interactions and the extent of organoclay exfoliation or intercalation in the molten state. Rheological measurements reflect the material's behavior in the melt state, while the morphological observations presented in our

Table 9. Mechanical properties of PP nanocomposites processed via the direct mixing method and two-step masterbatch.

Sample	Young's modulus ± SD (MPa)	Young's modulus improvement ± SD (%)	Yield strength ± SD (MPa)	Yield strength improvement ± SD (%)	Impact strength ± SD (kJ/m²)	Impact strength improvement ± SD (%)
PP	1481.4 ± 36.5	-	20.86 ± 0.09	-	15.99 ± 1.89	-
Nanocomposites processed via direct process method						
C11	1489.5 ± 26.9	0.6 ± 0.1	21.02 ± 0.24	0.77 ± 0.01	11.22 ± 0.48	-29.83 ± 3.75
C21	1504.8 ± 89.4	1.6 ± 0.1	21.10 ± 0.38	1.15 ± 0.02	8.96 ± 1.56	-43.96 ± 9.25
C31	1546.5 ± 44.6	4.4 ± 0.2	20.59 ± 0.66	-1.29 ± 0.04	9.06 ± 1.18	-43.34 ± 5.15
H11	1507.5 ± 60.6	1.8 ± 0.1	21.80 ± 0.23	4.51 ± 0.05	11.20 ± 1.40	-29.96 ± 5.15
H21	1595.3 ± 73.0	7.7 ± 0.4	21.68 ± 0.35	3.93 ± 0.07	9.43 ± 1.38	-41.03 ± 7.72
H31	1579.9 ± 92.3	6.7 ± 0.4	21.37 ± 0.19	2.44 ± 0.02	7.45 ± 1.82	-53.41 ± 14.49
Nanocomposites processed via two-step masterbatch method						
PC1	1597.7 ± 18.5	7.9 ± 2.9	22.05 ± 0.43	5.70 ± 2.11	7.84 ± 1.18	-50.97 ± 9.38
PC2	1684.8 ± 18.5	13.7 ± 3.1	22.03 ± 0.14	5.61 ± 0.81	7.92 ± 0.68	-50.47 ± 7.24
PC3	1638.4 ± 21.0	10.6 ± 3.1	21.94 ± 0.25	5.18 ± 1.28	9.31 ± 1.60	-41.78 ± 12.14
PC4	1632.6 ± 78.0	10.2 ± 5.9	21.22 ± 0.39	1.73 ± 1.92	8.67 ± 0.76	-45.78 ± 7.98
PC5	1647.4 ± 24.1	11.2 ± 3.2	21.78 ± 0.24	4.41 ± 1.24	9.67 ± 0.95	-39.52 ± 9.29

study are based on the solid-state microstructure, obtained after compounding and molding. It is well recognized that morphological rearrangements can occur during cooling and crystallization, particularly in semi-crystalline polymers like PP, which may lead to differences between melt-state dispersion and final solid-state structure [15]. While rheological data would certainly complement the understanding of nanoclay dispersion, we opted to focus on direct solid-state characterization methods such as XRD and SEM in this study. SEM micrographs are exhibited in Figure 8 and their relevant interpretation is explained.

The mechanical properties of the neat PP and its nanocomposites processed via direct method are reported in Table 9 and illustrated in Figure 4. According to Table 9 and Figure 4a, the maximum elastic moduli belong to C31 and H21 samples, for the C and H series, respectively. This observation confirms the already mentioned hypothesis that the best nanoclay dispersion has possibly occurred in these two samples. There is no significant difference between yield strength values of the samples and only slight changes are observed (Figure 4b). The nanocomposites exhibit up to 53% lower impact strength than the neat PP. Considering the higher elastic modulus of H21 compared to C31, the formulation of H21 was selected for the next part of the study where the influence of process sequence, i.e. incorporation of the compatibilizer in two steps will be examined.

Although the observed percentage changes in mechanical properties such as Young's modulus and yield strength were relatively modest (typically below 8%), statistical analysis using one-way ANOVA revealed that all p-values are well below the commonly used significance threshold of 0.05 ($p < 0.01$), indicating that there are statistically meaningful differences among the formulated systems for each of the mechanical properties tested. Several of these changes are comparable at the 95% confidence level. This is primarily due to the low standard deviations in the mechanical test data and the consistency across replicates. For instance, the neat PP exhibited a yield strength of 20.86 ± 0.09 MPa, while the H11 nanocomposite increased this to 21.80 ± 0.23 MPa. Despite the enhancement appearing small in absolute terms (~4.5%), the narrow variability in datasets resulted in non-overlapping confidence intervals. These findings emphasize the importance of combining statistical analysis with percentage change assessments, as even minor variations can have meaningful implications in polymer compound performance, especially when measurements are precise and reproducible.

The mechanical properties of the neat PP and its nanocomposites processed via the direct method are reported in Table 9 and illustrated in Figure 4. According to Table 9 and Figure 4a, the maximum elastic moduli belong to the C31 and H21 samples for the C and H series, respectively. This observation supports the earlier hypothesis that optimal nanoclay dispersion likely occurred in these two formulations. There is no significant difference between the yield strength values of the samples, and only slight variations are observed (Figure 4b). The nanocomposites exhibited up to 53% lower impact strength compared to neat PP. Considering the higher elastic modulus of H21 relative to C31, the H21 formulation was selected for the next stage of the study, where the influence of process

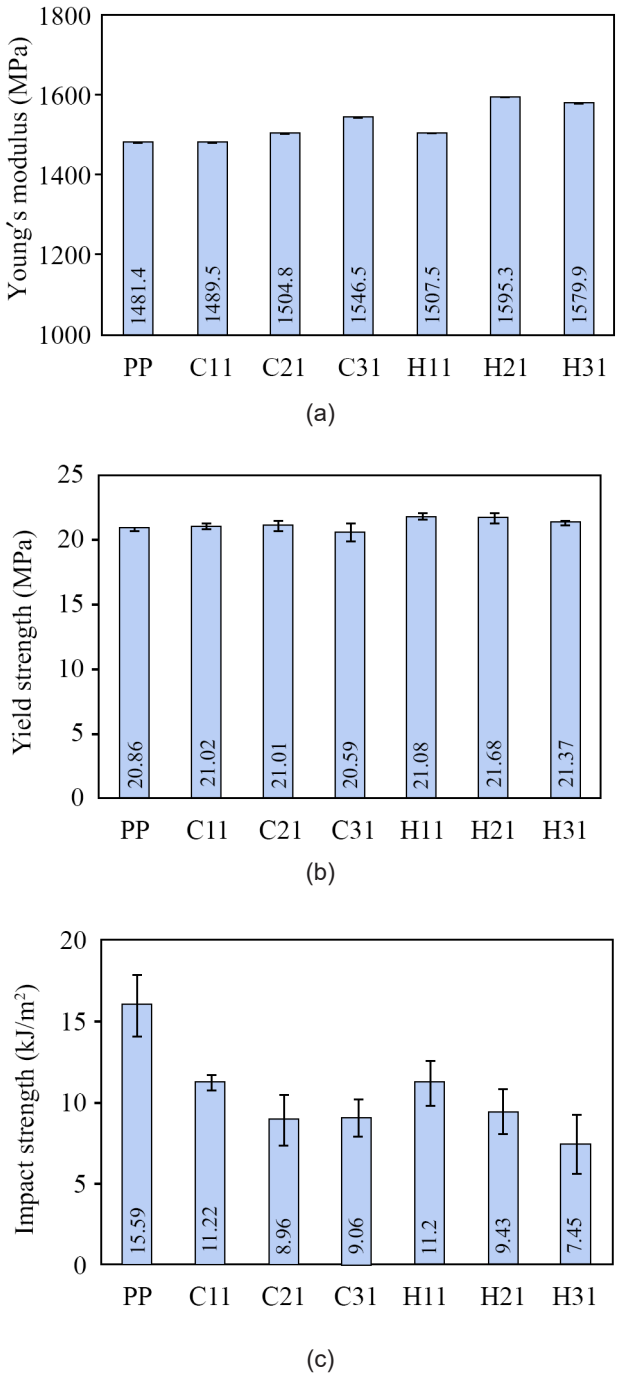

Figure 4. Mechanical properties of PP and its nanocomposites processed via the direct mixing method: (a) Young's modulus, (b) yield strength, and (c) impact strength. Each value is the average of at least five measurements per formulation.

sequence-i.e., incorporation of the compatibilizer in two steps-was investigated.

Although the observed changes in mechanical properties, such as Young's modulus and yield strength, were relatively modest (typically below 8%), statistical analysis using one-way ANOVA revealed that all p-values were well below the commonly accepted significance threshold of 0.05 ($p < 0.01$), indicating statistically meaningful differences among the formulated systems for each mechanical property tested. Several of these changes are comparable at the 95% confidence level. This is primarily attributed to the low standard deviations in the mechanical test data and the high consistency of replicates. For instance, the neat PP exhibited a yield strength of 20.86 ± 0.09 MPa, while the H11 nanocomposite increased this value to 21.80 ± 0.23 MPa. Although the enhancement appears small in absolute terms (~4.5%), the narrow variability in the datasets resulted in non-overlapping confidence intervals. These findings emphasize the importance of complementing percentage change assessments with statistical analysis, as even minor improvements can be meaningful in polymer compound performance when measurements are precise and reproducible.

A relatively high loading of PP-g-MA was required to achieve even partial improvements in nanocomposite properties. This can be attributed to the low grafting degree of the synthesized compatibilizers, as evidenced by titration results and MA content measurements (Table 6). Due to the limited number of functional groups available for interaction with the clay surface, a larger quantity of compatibilizer was necessary to promote dispersion and interfacial adhesion. However, despite this substantial loading, the enhancements in mechanical and thermal properties remained modest. This suggests that the compatibilization mechanism was not fully effective, potentially due to insufficient graft density or suboptimal molecular architecture of the grafted chains.

Previous studies have shown that not only the MA content but also the distribution and length of grafted chains on the PP backbone significantly influence compatibilizer efficiency [7,28]. For instance, short-chain grafts may fail to anchor effectively onto clay surfaces, while excessively long grafted segments may preferentially entangle with the matrix, reducing interaction with the filler. Moreover, high polydispersity and random grafting sites can result in steric hindrance or ineffective surface coverage [29]. These findings highlight the importance of optimizing the grafting process-not only to increase the grafting degree but also to tailor the structure and reactivity of PP-g-MA for more efficient interfacial interaction with nanofillers.

Effect of process sequence

Figure 5 depicts the XRD patterns of samples processed via the two-step method. Composition of all the samples was identical to H21 (3 wt.% of nanoclay and 6 wt.%

of HPP-g-MA). The interlayer spacings of organoclay particles after two-step process are given in Table 10. Compared to H21 ($\bar{d}$ 35.88 Å), all the samples had larger interlayer spacing ($\bar{d}$=37.25-38.89 Å), and therefore, it can be concluded that the two-step method has effectively enhanced the intercalation. However, these improvements did not follow a specific trend and PC5, in which all the compatibilizers were incorporated in the first step ($\bar{d}$ =38.89Å , demonstrated the highest increase in interlayer spacing ($\bar{d}/\bar{d}_{DK4}\times100$=9.7). Considering the constant concentration of nanoclay in each of five samples and the peak of 2θ = 9.5°, which is related to base polymer and has an identical intensity for all the samples, partial exfoliation might have happened for PC1 and PC2 on larger scales owing to the lower peak intensities. According to Figure 5, there is a noticeable decrease in the intensity of the characteristic peaks from samples PC5 to PC1, which suggests some degree of clay exfoliation in samples PC1 and PC2. A reduction in peak intensity implies a possible degree of exfoliation in combination with intercalation; presumably, the lower the peak intensity, the greater the extent of nanoclay exfoliation. Thus, TEM assessments are essential for validating the partial exfoliation of clay platelets within the matrix.

Young's modulus, yield strength and impact strength of five samples prepared by a two-step method, H21 and base polymer of nanocomposites (PP), along with their propagated standard deviations are reported in Table 9 and plotted in Figure 6. Generally, the mechanical properties of two-step processed samples are expected to be improved. However, it is obvious that they did not show any significant changes in Young's modulus, yield strength and impact strength with respect to H21, even PC1 and PC2 with higher portions of exfoliated or massive intercalated organoclay structures. These results are probably due to the fact that poor mechanical properties of masterbatch base polymer, 548T CPP with MFI of

Table 10. XRD results for nanocomposites processed via the two-step masterbatch method.

Sample	$\overline{2\theta}$ (°)	$\bar{d}$(Å)	$\bar{d}/\bar{d}_{DK4}\times100$
DK4	2.49	35.45	0
H21	2.46	36.88	1.21
PC1	2.37	37.25	5.08
PC2	2.36	37.41	5.53
PC3	2.30	38.38	8.27
PC4	2.31	38.21	7.79
PC5	2.27	38.89	9.70

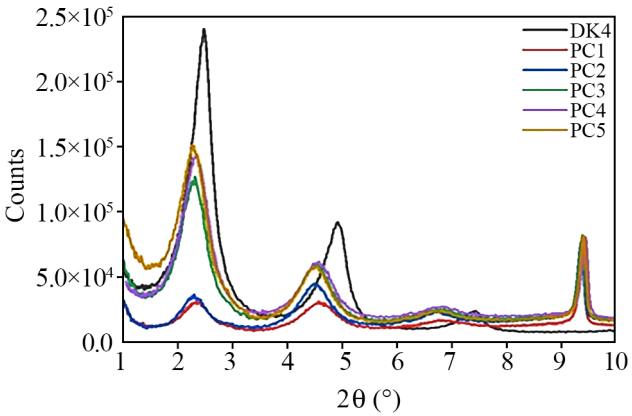

Figure 5. XRD patterns of nanocomposites processed via the two-step masterbatch method.

50 g/10 min is overlooked. 548T has a relatively low Young's modulus and yield strength compared to EP440L (main base polymer) and consequently, its marked negative effect on final properties can be seen. Dang and Bhattacharyya [14] explained that an excess amount of compatibilizer within the matrix can lead to the plasticization of the matrix, thereby challenging the influence of morphology on the mechanical properties of clay-PP nanocomposites.

Furthermore, as discussed earlier, the high loading of PP-g-MA required to achieve partial improvements may also be linked to the low grafting efficiency of the synthesized compatibilizer. Despite significant amounts of PP-g-MA, the limited degree of functionalization likely restricted effective interfacial interactions with clay, thereby reducing the potential reinforcement effects of the improved morphology. This inefficiency in the compatibilization mechanism further explains the marginal gains in mechanical properties observed in the two-step processed samples.

The mechanical properties of the neat PP and its various nanocomposite formulations, reported in Table 9, were statistically analyzed using one-way ANOVA followed by Tukey's post hoc test. The analysis revealed that the observed differences in Young's modulus, yield strength and impact strength among the compatibilized nanocomposites were statistically significant within the experimental variation ($p < 0.005$), particularly for H21, PC2, and PC5 compared to the neat PP, even though some percent changes appeared modest or even small. This statistical outcome supports the reliability of the experimental differences as a result of the compatibilizer and organoclay addition.

To evaluate the effect of compatibilizer and base polymer of masterbatches, two additional samples,

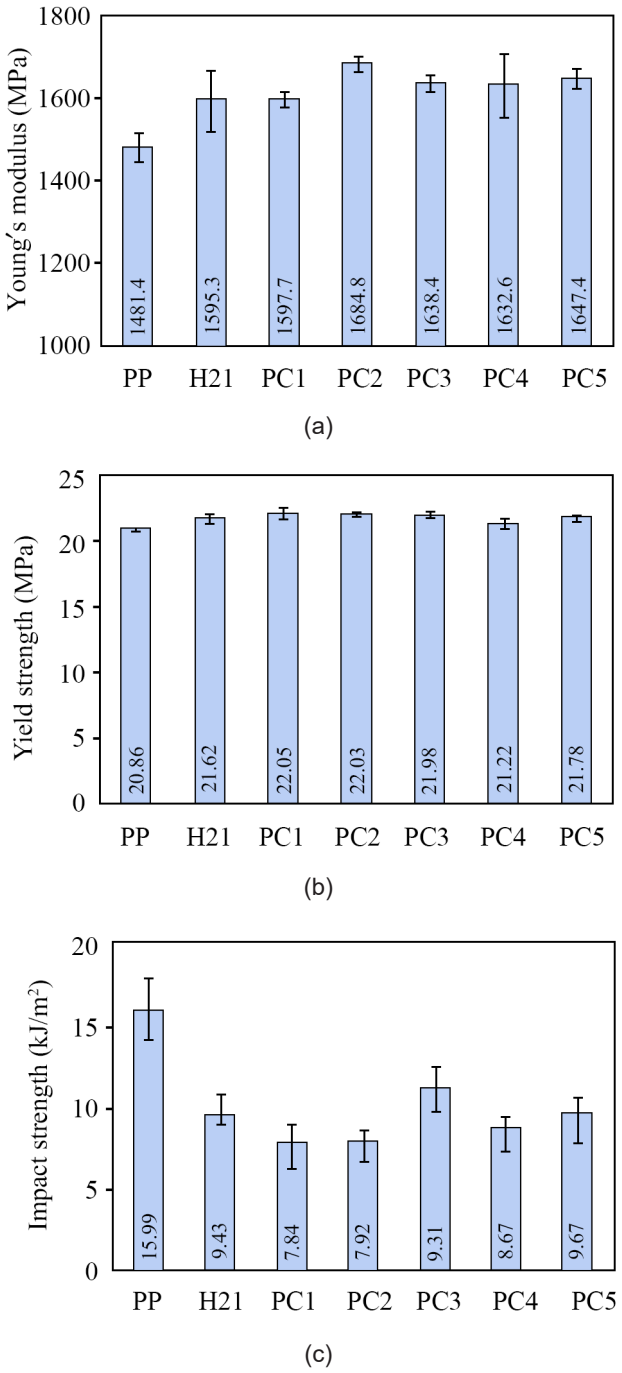

Figure 6. Mechanical properties of PP and its nanocomposites processed via the two-step masterbatch method:(a) Young's modulus, (b) yield strength, and (c) impact strength. Each value represents the average of at least five measurements per formulation.

namely PP+HPP-g-MA and PP+PP-MB, were processed and characterized. Table 11 describes the compositions of these two formulated compounds and reports the mechanical properties of these formulations. According to the table, PP+HPP-g-MA is a compound of EP440L co-PP and 6 wt.% of HPP-g-MA compatibilizer similar to the composition of the nanocomposites processed using direct process. As mentioned in the experimental section, PP+PP-MB containing 12 wt.% of 548T was prepared to characterize the effect of masterbatches' base polymer on the mechanical properties of the nanocomposites studied in this investigation. According to Table 11, incorporation of the compatibilizer to the base polymer reduced Young's modulus from 1481.4 MPa to 1448.2 MPa. The incorporation of 12 wt.% 548T co-PP into the matrix, EP440L co-PP, resulted in a decrease in Young's modulus from 1481.4 MPa to 1343.6 MPa. The trace of the base polymer of masterbatch was eliminated (proportional to the amount of incorporated 548T in the corresponding sample) and the resulting values were compared with PP+HPP-g-MA as the reference sample in Table 11. Be mentioned that it is clear that decreasing the compatibilizer content in the first step results in higher values of Young's modulus. Table 11 also provides information about yield strength and impact strength of samples after the elimination of traces of masterbatch base polymer. Similarly, the values were compared with the value of the reference sample, PP+HPP-g-MA. It can be concluded that a decline in compatibilizer content in the first step of processing leads to higher increases in yield strength and higher decreases in impact strength.

Finally, SEM micrographs taken from the fracture surfaces of the PP, H21, and PC1 specimens after impact loading are exhibited in Figure 7. Figure 7a shows a two-phase microstructure for the neat co-polypropylene, EP440L, as expected. EP440L is a heterophasic copolymer, as explicitly stated in its technical datasheet. This type of polymer typically consists of a semi-crystalline PP matrix with a dispersed ethylene-propylene rubber (EPR) phase, introduced to improve impact properties. The presence of this rubber phase leads to morphological contrast under SEM, where the bright spherical domains and associated cavities are consistent with rubber-rich domains [13].

In Figure 7, corresponding to H21 and PC1, distinct spherical or droplet-like features are also observed within the PP matrix. These droplets, now marked with arrows in the revised figure, are attributed to the rubbery domains inherent in the copolymer matrix and remain visible even in the presence of nanofillers. Their presence indicates that the intrinsic two-phase morphology of the matrix is largely retained upon nanoclay addition. In H21 (Figures 7b and 7d), large organoclay aggregates can also be seen, suggesting the presence of non-exfoliated or partially intercalated

Table 11. Effect of compatibilizer and masterbatch base polymer on the mechanical properties of nanocomposites processed via the two-step masterbatch method.

Designation	Young's modulus ± SD (MPa)	Modulus [1] ± SD (MPa)	% Change in modulus [2]	Yield [1] strength ± SD (MPa)	Yield strength (MPa)	% Change in yield strength[2]	Impact strength ± SD (kJ/m²)	Impact strength [1] ± SD (kJ/m²)	% Change in impact strength [2]
PP	1481.4 ± 36.5	-	-	20.86 ± 0.09	-	-	15.99 ± 1.89	-	-
PP-HPP-g-MA[3]	1448.2 ± 63.2	-	-	21.18 ± 0.27	-	-	13.12 ± 1.18	-	-
PP-PP-MB[4]	1343.6 ± 58.9	-	-	19.99 ± 0.64	-	-	15.46 ± 1.46	-	-
H21	1595.3 ± 73.0	-	10.16	21.68 ± 0.35	-	2.36	9.43 ± 1.38	-	28.13
PC1	1597.7 ± 18.5	1746.3 ± 61.9	20.58	22.05 ± 0.43	22.92 ± 0.71	8.22	7.84 ± 1.18	8.42 ± 1.92	35.82
PC2	1684.8 ± 18.5	1799.6 ± 61.9	24.26	22.03 ± 0.14	22.75 ± 0.66	7.41	7.92 ± 0.68	8.40 ± 1.61	35.98
PC3	1638.4 ± 21.0	1741.7 ± 62.4	20.27	21.94 ± 0.25	22.59 ± 0.68	6.66	9.31 ± 1.60	9.74 ± 2.17	25.76
PC4	1632.6 ± 78.0	1724.4 ±100.8	19.07	21.22 ± 0.39	21.80 ± 0.75	2.93	8.67 ± 0.76	9.06 ± 1.63	30.95
PC5	1647.4 ± 24.1	1716.3 ± 63.4	18.51	21.78 ± 0.24	22.21 ± 0.68	4.86	9.67 ± 0.95	9.96 ± 1.74	24.09

[1]After eliminating the effect of masterbatch based polymer

[2] compared to PP-HPP-g-MA

[3]PP-HPP-g-MA: 94 wt.% EP440L co-PP + 6 wt.% HPP-g-MA

[4]PP-PP-MB: 88 wt.% EP440L co-PP + 12 wt.% 548T co-PP

stacks. In contrast, PC1 (Figures 7c and 7e) displays a finer dispersion of organoclay, including both intercalated and exfoliated structures. Moreover, pulled-out nanoclay stacks are observed in both H21 and PC1, indicating weak interfacial adhesion between the filler and the matrix. As the compatibilizer is expected to be located at this interface, the observed adhesion quality is closely related to the nature and efficiency of the compatibilizer employed.

Figure 7f displays the microstructure of homo-PP, which lacks the rubbery droplets seen in the co-PP matrix, further confirming the attribution of these spherical domains to the EPR phase in the copolymer.

CONCLUSION

To summarize, two types of PP-based compatibilizer

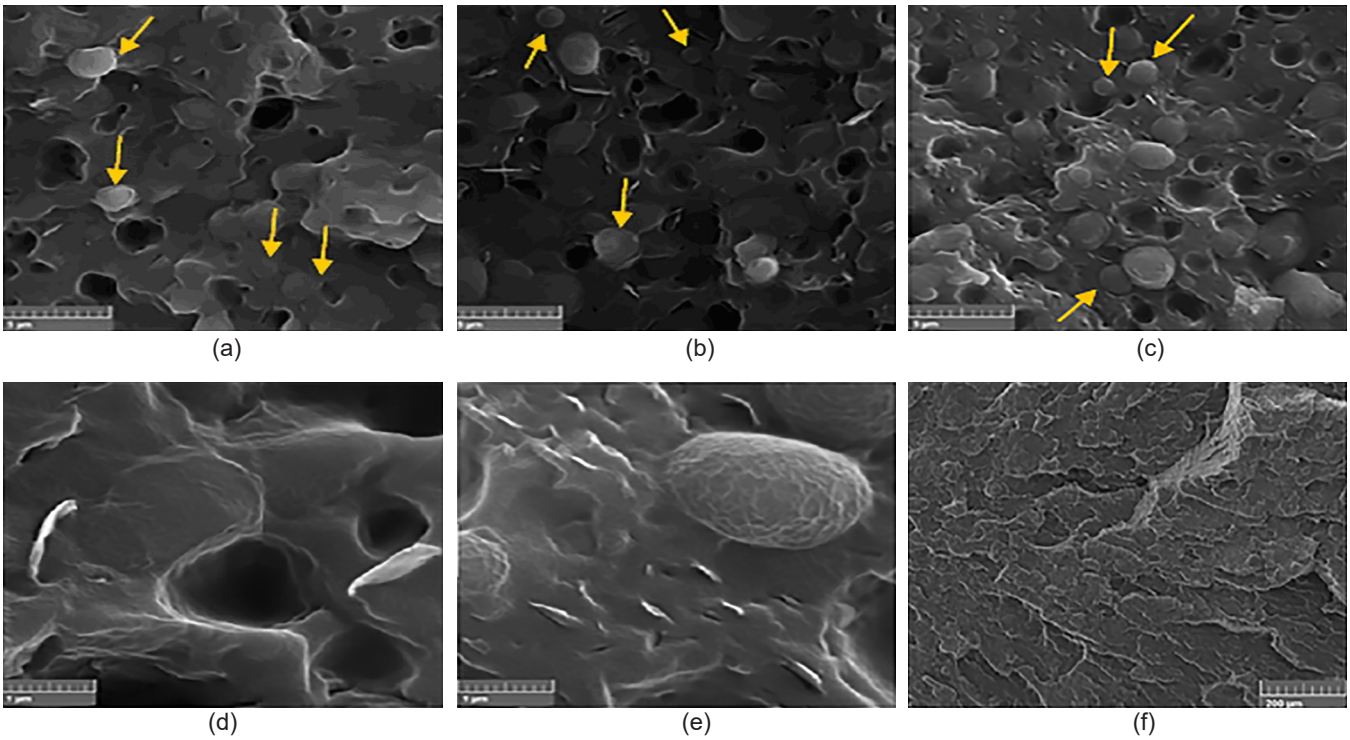

Figure 7. SEM micrographs of fracture surfaces after impact testing for (a) co-PP, (b,d) H21, (c,e) PC1 and (f)homo-PP. Arrows indicate rubbery EPR domains dispersed in the matrix, retained from the original copolymer structure. Organoclay stacks, including some pulled-out platelets, are also visible, particularly in H21, suggesting non-exfoliated stacks. Improved dispersion is observed in PC1.

were synthesized and characterized using titration, MFI, FTIR and frequency sweep tests. Both compatibilizers were incorporated into nanocomposite samples with different concentrations. HPP-g-MA surpassed CPP-g-MA in overall mechanical properties, and the overall ranking suggests that H21 (HPP-g-MA:nanoclay ratio of 2:1) is the best sample among all. Regarding the samples fabricated by the two-step method, although better exfoliation and dispersion of nanoclay platelets were observed, due to the poor properties of masterbatches' base polymer, no significant improvement in mechanical properties was achieved.

ACKNOWLEDGEMENTS

The authors would like to thank Parsa Polymer Company for test specimen preparation. The authors would also like to express gratitude to Prof. Ashuri and Ms. Rohani at Sharif University of Technology for their valuable help during this project.

CONFLICTS OF INTEREST

The authors declare no competing interests.

REFERENCES

1. Chafidz A, Faisal R, Kaavessina M, Hartanto D (2018) Non-isothermal crystallization and viscoelastic behavior of polypropylene/nanoclay composites fabricated from masterbatch by using a mini extruder. Defect Diffus Forum 382: 89-93
2. Shokrollahi M, Marouf BT, Bagheri R (2022) Role of the nucleating agent masterbatch carrier resin in the nonisothermal crystallization kinetics of polypropylene. Polymer J 54: 1127-1132
3. Hiziroglu HR, Shkolnik IE (2018) Electrical characteristics of polypropylene mixed with natural nanoclay. Polymers 10: 942
4. Taktak S, Fakhfakh S, Rondot S, Tara A, Jbara O (2022) Behavior under electron irradiation of two clay-based polymer nanocomposites PPgMA/OMMT and PBS/OMMT. Mater Chem Phys 275: 125230
5. Blazquez M, Marchante V, Gendre L, Starost K, Njuguna J, Schutz JA, Lacave JM, Egizabal A, Elizetxea C, Cajaraville MP (2020) Particle emission measurements in three scenarios of mechanical degradation of polypropylene-nanoclay nanocomposites. J Aerosol Sci 150: 105629
6. Pettarin V, Brun F, Viana JC, Pouzada AS, Frontini PM (2013) Toughness distribution in complex PP/nanoclay injected mouldings. Compos Sci Technol 74: 28-36
7. Paul D, Robeson L (2008) Polymer nanotechnology: Nanocomposites. Polymer 49: 3187-3204
8. Kotal M, Bhowmick AK (2015) Polymer nanocomposites from modified clays: Recent advances and challenges. Prog Polym Sci 51: 127-187
9. López-Quintanilla ML, Sánchez-Valdés S, Ramos de Valle LF, Medellín-Rodríguez FJ (2006) Effect of some compatibilizing agents on clay dispersion of polypropylene-clay nanocomposites. J Appl Polym Sci 100: 4748-4756
10. Abacha N, Fellahi S (2005) Synthesis of polypropylene-graft-maleic anhydride compatibilizer and evaluation of nylon 6/ polypropylene blend properties. Polymer Int 54: 909-916
11. Pruthtikul R, Liewchirakorn P (2010) Preparation of polypropylene graft maleic anhydride (PP-g-MA) via twin screw extrusion. Adv Mater Res 93-94: 451-454
12. Güldoğan Y, Eğri S, Rzaev ZMO, Pişkin E (2004) Comparison of maleic anhydride grafting onto powder and granular polypropylene in the melt by reactive extrusion. J Appl Polym Sci 92: 3675-3684
13. Zhang C, Shangguan Y, Chen R, Wu Y, Chen F, Zheng Q, Hu G (2010) Morphology, microstructure and compatibility of impact polypropylene copolymer. Polymer 51: 4969-4977
14. Krishnamoorti R, Vaia RA (2001) Polymer nanocomposites: synthesis, characterization and modeling, Vol. 804, ACS Publications
15. Krishnamoorti R, Vaia RA (2007) Polymer nanocomposites. J Polym Sci Pol Phys 45: 3252-3256
16. Baniasadi H, Ramazani SA A, Javan Nikkhah S (2010) Investigation of in situ prepared polypropylene/clay nanocomposites properties and comparing to melt blending method. Mater Des 31: 76-84

17. López-Quintanilla M, Sánchez-Valdés S, Ramos de Valle L, Guedea Miranda R (2006) Preparation and mechanical properties of PP/PP-g-MA/Org-MMT nanocomposites with different MA content. Polym Bull 57: 385-393
18. Pascual J, Fages E, Fenollar O, García D, Balart R (2009) Influence of the compatibilizer/nanoclay ratio on final properties of polypropylene matrix modified with montmorillonite-based organoclay. Polym Bull 62: 367-380
19. Chafidz A, Ali MA, Elleithy R (2011) Morphological, thermal, rheological, and mechanical properties of polypropylene-nanoclay composites prepared from masterbatch in a twin screw extruder. J Mater Sci 46: 6075-6086
20. Shroff Rama M, Neppalli R, Chellaswamy R, Swaminathan S (2010) Exfoliation of clay layers in polypropylene matrix using potassium succinate-g-polypropylene as compatibilizer. Compos Sci Technol 70: 1550-1556
21. Nam BU, Son Y (2010) Evaluations of PP-g-GMA and PP-g-HEMA as a compatibilizer for polypropylene/clay nanocomposites. Polym Bull 65: 837-847
22. Rodríguez-Llamazares S, Rivas BL, Pérez M, Perrin-Sarazin F, Maldonado A, Venegas C (2011) The effect of clay type and of clay–masterbatch product in the preparation of polypropylene/clay nanocomposites. J Appl Polym Sci 122: 2013-2025
23. Nguyen VK, Jin SH, Lee SH, Lee DS, Choe S (2006) Polypropylene/clay nanocomposites prepared with masterbatches of polypropylene ionomer and organoclay. Compos Interfaces 13: 299-310
24. Darestani Farahani A (2013) Mechanical and microstructural evaluations of (high MFI PP/low MFI PP)/organoclay nanocomposites influence of clay loading, compatibilizer loading and processing, Master Thesis, Sharif University of Technology
25. Moad G (1999) The synthesis of polyolefin graft copolymers by reactive extrusion. Prog Polym Sci 24: 81-142
26. Oromehie AR, Hashemi SA, Meldrum IG, Waters DN (1997) Functionalisation of polypropylene with maleic anhydride and acrylic acid for compatibilising blends of polypropylene with poly(ethylene terephthalate). Polym Int 42: 117-120
27. Beyler CL, Hirschler MM (2002) Thermal decomposition of polymers. SFPE handbook of fire protection engineering 2, Section 1, Chapter 7, 111-131
28. Tjong SC (2006) Structural and mechanical properties of polymer nanocomposites. Mater Sci Eng: R: Reports 53: 73-197
29. Zanetti M, Camino G, Thomann R, Mülhaupt R (2001) Synthesis and thermal behaviour of layered silicate–EVA nanocomposites. Polymer 42: 4501-4507